Backbone Flexibility and Counterion Effects on the Structure and Thermal Properties of Di(thiourea)zinc Dicarboxylate Coordination Polymers

Andrew D. Burrows,*[a] Adele S. Donovan,[a] Ross W. Harrington,[a] and Mary F. Mahon[a]

Keywords: Crystal engineering / Coordination polymers / Helical structures / Hydrogen bonds / Zinc

The reaction between $[Zn(tu)_4]Cl_2$ and the appropriate sodium dicarboxylate has been shown to give the coordination polymers $[Zn(tu)_2(\mu\text{-succinate})]_n$ (**7**), $[Zn(tu)_2(\mu\text{-itaconate})]_n$ (**8**), $[Zn(tu)_2(\mu\text{-ethylmalonate})]_n$ (**9**), $[Zn(tu)_2(\mu\text{-1,3-phenylenediacetate})]_n$ (**10**) and $\{[Zn(tu)_2(\mu\text{-mesaconate})]\cdot 2H_2O\}_n$ (**11**), all of which have been crystallographically characterised. The crystal structures of **7**–**9** demonstrate that these compounds form helical structures in which the dicarboxylates adopt conformations with the relative positions of the carboxylate groups similar to those in constrained anions such as phthalate. The role of the chloride counterion in the starting material has been explored by investigating the reactions of $[Zn(tu)_4](NO_3)_2$ with a range of dicarboxylates. Although in the majority of cases the counterion was shown to have no effect, in the case of fumarate, a hydrated coordination polymer $\{[Zn(tu)_2(\mu\text{-fumarate})]\cdot 2H_2O\}_n$ (**12**) was observed in addition to the anhydrous product $[Zn(tu)_2(\mu\text{-fumarate})]_n$ (**1**), which was formed as the sole product from $[Zn(tu)_4]Cl_2$. Thermogravimetric analyses are reported for compounds **1**–**12**. The compounds $\{[Zn(tu)_2(\mu\text{-isophthalate})]\cdot H_2O\}_n$ **3** and **12** lose their included water before 140 °C, whereas the compounds $\{[Zn(tu)_2(\mu\text{-maleate})]\cdot H_2O\}_n$ **6** and **11** only lose their water molecules at higher temperatures with the onset of decomposition. This difference in behaviour can be related to the structural role of the water molecules.

Introduction

The majority of crystal engineering studies employ one of two strategies to engender structural predictability. Hydrogen bonds, especially in systems involving two or more such interactions between the same molecules or ions, have proved effective in both organic and inorganic systems.[1−3] In the latter, bifunctional ligands containing both coordination sites and hydrogen-bonding faces are used to include metal centres.[4] A number of examples of bifunctional ligands have been reported recently, including bis(imidazolates),[5] amidinoureas[6] and oxalurates.[7] Inorganic crystal engineering has also exploited coordination bonds in the formation of metal-organic frameworks.[8−10] This approach relies on the use of polytopic ligands that are able to bridge between metal centres. Bridging coordination modes are encouraged through rigidity in the ligand, which makes chelation geometrically impossible.

We have been interested in the interplay between the hydrogen bond and coordination bond approaches, and have focussed attention on systems in which both types of aggregation are possible and potentially in competition.[11−13] We recently reported the reactions of $[Zn(tu)_4]Cl_2$ with the appropriate sodium dicarboxylates to give the coordination polymers $[Zn(tu)_2(\mu\text{-fumarate})]_n$ (**1**), $[Zn(tu)_2(\mu\text{-malonate})]_n$ (**2**), $\{[Zn(tu)_2(\mu\text{-isophthalate})]\cdot H_2O\}_n$ (**3**), $[Zn(tu)_2(\mu\text{-phthalate})]_n$ (**4**), $[Zn(tu)_2(\mu\text{-citraconate})]_n$ (**5**) and $\{[Zn(tu)_2(\mu\text{-maleate})]\cdot H_2O\}_n$ (**6**).[14] In all cases, the coordination polymers are interconnected through hydrogen bonds, and these are dominated by interactions involving the thiourea face containing two parallel NH groups. Similar observations on zinc and cadmium dicarboxylates have been reported by Zhang and co-workers.[15−17]

In this paper we extend the reaction between $[Zn(tu)_4]Cl_2$ and dicarboxylate to a further five anions. In three of these − succinate, itaconate and 1,3-phenylenediacetate − there is much greater conformational flexibility due to the inclusion of one or more sp^3-hybridised carbon atoms between the carboxylate groups. Ethylmalonate and mesaconate were chosen to determine the structural effects of alkyl substituents by comparison with the previously reported malonate and fumarate compounds. We report herein the crystal structures of the products $[Zn(tu)_2(\mu\text{-succinate})]_n$ (**7**), $[Zn(tu)_2(\mu\text{-itaconate})]_n$ (**8**), $[Zn(tu)_2(\mu\text{-ethylmalonate})]_n$ (**9**), $[Zn(tu)_2(\mu\text{-1,3-phenylenediacetate})]_n$ (**10**) and $\{[Zn(tu)_2(\mu\text{-mesaconate})]\cdot 2H_2O\}_n$ (**11**), and compare their supramolecular structures with those previously reported for compounds **1**−**6**. The role of the counterion in the starting material has also been explored by investigating the reactions of $[Zn(tu)_4](NO_3)_2$ with a range of dicarboxylates. This has led to the structural characterisation of $\{[Zn(tu)_2(\mu$-

[a] Department of Chemistry, University of Bath, Claverton Down, Bath BA2 7AY, UK
Fax: (internat.) + 44-1225-386231
E-mail: a.d.burrows@bath.ac.uk

Supporting information for this article is available on the WWW under http://www.eurjic.org or from the author.

  DOI: 10.1002/ejic.200400502

fumarate)]·2H_2O}$_n$ (**12**). The dicarboxylates relevant to this paper are illustrated in Scheme 1.

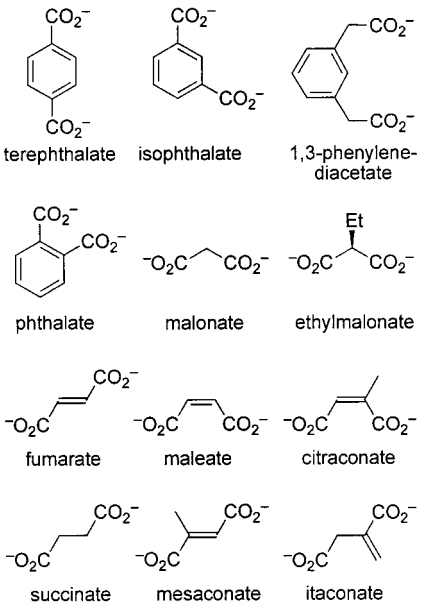

Scheme 1. Dicarboxylates incorporated in compounds **1**−**12** or mentioned in the text

Syntheses of Compounds 7−11

Compounds **7**−**11** were prepared from the reaction between [Zn(tu)$_4$]Cl$_2$ and the appropriate sodium dicarboxylate in water; crystallisation typically occurred over a period of a week. Yields were in the range 51−78%. In each case, crystals suitable for single-crystal analysis were obtained and the representative nature of the single crystals chosen for analyses to the bulk materials were confirmed by comparison of the X-ray powder diffraction pattern with that predicted from the single-crystal data. The compounds were identified as [Zn(tu)$_2$(μ-succinate)]$_n$ (**7**), [Zn(tu)$_2$(μ-itaconate)]$_n$ (**8**), [Zn(tu)$_2$(μ-ethylmalonate)]$_n$ (**9**), [Zn(tu)$_2$(μ-1,3-phenylenediacetate)]$_n$ (**10**) and {[Zn(tu)$_2$(μ-mesaconate)]·2H_2O}$_n$ (**11**). The structures of **7**−**11** are all based on coordination polymers, and the Zn(tu)$_2$ centres are bridged by dicarboxylate ligands. In all cases, the zinc centres adopt distorted tetrahedral coordination geometries. However, variation in the relative orientations of the carboxylate groups within the individual dicarboxylates leads to differences in the conformations of the polymer chains and in the manner in which they interact with each other. Selected bond lengths and angles for compounds **7**−**11** are given in Tables 1 and 2.

Table 2. Selected bond lengths and angles for compound **10**; primed atoms generated by the symmetry transformation $-x$, $y - {}^1/_2$, $-z + {}^1/_2$; double-primed atoms generated by the symmetry transformation $-x + 1$, $y - {}^1/_2$, $-z + {}^1/_2$

Zn(1)−S(1)	2.3268(7)	Zn(2)−S(3)	2.3374(7)
Zn(1)−S(2)	2.3337(7)	Zn(2)−S(4)	2.3047(6)
Zn(1)−O(2)	1.9833(17)	Zn(2)−O(6)	1.9686(17)
Zn(1)−O(4)′	1.9629(17)	Zn(2)−O(8)"	1.9849(18)
S(1)−Zn(1)−S(2)	102.96(2)	S(3)−Zn(2)−S(4)	117.55(2)
S(1)−Zn(1)−O(2)	108.50(5)	S(3)−Zn(2)−O(6)	107.63(5)
S(1)′−Zn(1)−O(4)′	110.56(6)	S(3)−Zn(2)−O(8)"	104.06(5)
S(2)−Zn(1)−O(2)	106.52(5)	S(4)−Zn(2)−O(6)	111.24(5)
S(2)−Zn(1)−O(4)′	132.79(5)	S(4)−Zn(2)−O(8)"	118.60(5)
O(2)−Zn(1)−O(4)′	93.49(7)	O(6)−Zn(2)−O(8)"	95.08(7)
Zn(1)−S(1)−C(12)	107.62(9)	Zn(2)−S(3)−C(23)	108.91(9)
Zn(1)−S(2)−C(11)	114.06(9)	Zn(2)−S(4)−C(24)	110.33(8)

The Structures of [Zn(tu)$_2$(μ-succinate)]$_n$ (7), [Zn(tu)$_2$(μ-itaconate)]$_n$ (8) and [Zn(tu)$_2$(μ-ethylmalonate)]$_n$ (9)

Compounds **7**, **8** and **9** each crystallise in space group $P2_12_12_1$ with lattice parameters within a narrow range. As their structures are broadly similar, they can be treated together. Compounds **7**−**9** all form helical coordination polymers, which propagate along the crystallographic *b* axes. The helices pack in hexagonal arrays, and within each structure, the chains all display the same handedness. In each case, intrachain hydrogen bonding between thiourea NH groups and carboxylate oxygen atoms is observed around the zinc centres. In compounds **7** and **8** there are two hydrogen bonds around each zinc centre, one involving a coordinated oxygen atom and the other involving an uncoordi-

Table 1. Selected bond lengths and angles for compounds **7**, **8**, **9**, **11** and **12**

	7[a]	**8**[b]	**9**[c]	**11**	**12**
Zn(1)−S(1)	2.3054(13)	2.3249(15)	2.313(2)	2.3329(12)	2.3322(12)
Zn(1)−S(2)	2.3269(14)	2.2948(15)	2.352(2)	2.3196(12)	2.3452(13)
Zn(1)−O(1)	1.999(3)	2.008(3)	1.985(5)	1.987(3)	1.980(3)
Zn(1)−O(3)	2.001(3)	1.999(4)	1.993(5)	2.002(3)	1.963(3)
S(1)−Zn(1)−S(2)	117.49(6)	119.51(6)	117.15(11)	117.68(5)	106.26(5)
S(1)−Zn(1)−O(1)	112.02(10)	119.58(11)	115.71(16)	104.36(10)	108.32(10)
S(1)−Zn(1)−O(3)	104.66(12)	103.49(10)	109.20(17)	107.64(10)	113.74(11)
S(2)−Zn(1)−O(1)	117.60(11)	108.21(11)	102.90(17)	105.83(10)	103.33(11)
S(2)−Zn(1)−O(3)	106.60(10)	108.25(11)	94.57(16)	116.74(11)	107.97(10)
O(1)−Zn(1)−O(3)	94.67(14)	93.79(15)	115.6(3)	102.73(13)	116.26(14)
Zn(1)−S(1)−C(1)	109.73(17)	107.95(19)	105.6(3)	109.84(16)	108.26(17)
Zn(1)−S(2)−C(2)	107.0(2)	108.14(19)	110.5(3)	109.20(17)	106.7(2)

[a] O(1) generated by the symmetry transformation $-x + 1$, $y + {}^1/_2$, $-z + {}^1/_2$. [b] O(3) generated by the symmetry transformation $-x + 1$, $y + {}^1/_2$, $-z + {}^3/_2$. [c] O(1) generated by the symmetry transformation $-x + 1$, $y - {}^1/_2$, $-z + {}^1/_2$.

nated oxygen atom. These hydrogen bonds give rise to S(6) and S(8) motifs, respectively, using graph set notation[18] (Figure 1). In both cases, the hydrogen bond leading to the six-membered ring involves the shorter N···O distance. The two Zn−S distances differ significantly (Table 1); the bond length involving the sulfur atom of the S(6) ring is longer than that of the S(8) ring. In compound **9**, there are also two hydrogen bonds present around each zinc centre, although in this case, both involve coordinated oxygen atoms as acceptors and consequently both result in the formation of S(6) rings.

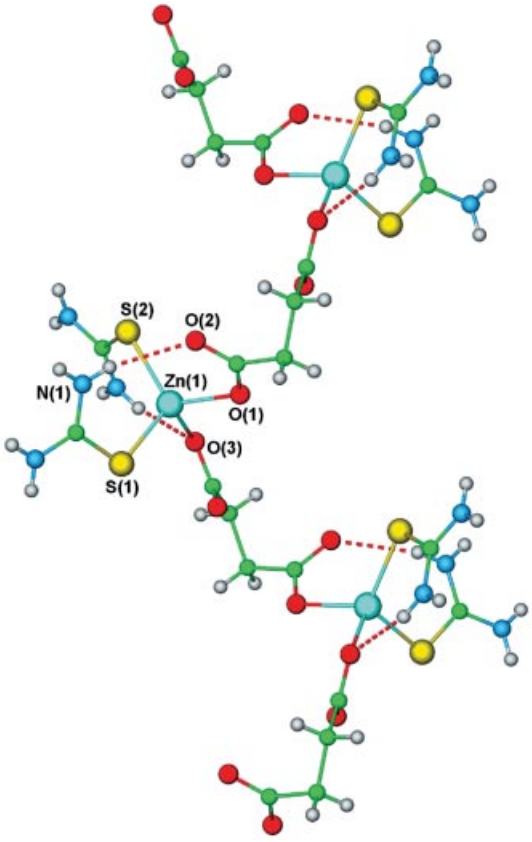

Figure 1. Intrachain hydrogen bonding in $[Zn(tu)_2(\mu\text{-succinate})]_n$ (**7**); selected hydrogen-bond lengths (Å) and angles (°) N(1)···O(2) 3.149, H(1B)···O(2) 2.33, N(1)−H(1B)···O(2) 161; and N(3)···O(3) 2.870, H(3B)···O(3) 2.20, N(3)−H(3B)···O(3) 165

In the helices, the Zn···Zn···Zn angles lie in a narrow range spanning 93° to 101°, and the Zn···Zn distances are 7.36 Å for **7**, 7.62 Å for **8** and 7.40 Å for **9**. Surprisingly the closest Zn···Zn distance occurs in the succinate compound **7** rather than its ethylmalonate analogue **9**, which has one less carbon atom between the carboxylate groups.

Further similarities between the three structures are evident with respect to the manner in which the helices interact together. In **7** and **8** the interactions are identical, occurring in two directions, corresponding to the crystallographic *a* and *c* axes. In each direction there are three independent hydrogen bonds, two of these involving the parallel NH groups on a thiourea ligand. A DD−AA interaction involving two hydrogen bonds between the parallel NH groups and two oxygen atoms generates $R_2^2(11)$ rings in the *a* direction (Figure 2). The two hydrogen-bond acceptors lie on the same dicarboxylate; one is coordinated and the other is uncoordinated. A further hydrogen bond involving an uncoordinated oxygen atom on a second dicarboxylate, generating a second $R_2^2(11)$ ring, completes the hydrogen bonding in this direction. The hydrogen bonding in the *c* direction is somewhat different as a single uncoordinated oxygen atom acts as acceptor to the two parallel NH groups, generating a $R_2^1(6)$ ring, although one of these interactions is relatively long in **7**. The final hydrogen bond in this direction involves a coordinated oxygen atom of a second dicarboxylate as acceptor, and generates a $R_2^2(11)$ ring motif. In each case, the hydrogen bonding is reciprocal along the crystallographic *a* axis, whereby each chain acts as a hydrogen-bond donor *and* acceptor to each adjacent chain, whereas along the crystallographic *c* axis the chains act as either hydrogen-bond donors *or* acceptors to each adjacent chain.

The interactions in **9** are broadly similar to those in **7** and **8**, although there are subtle differences. In the *a* direction, the acceptors for the parallel NH groups are both uncoordinated, generating a $R_2^2(10)$ motif, whereas the third hydrogen bond is to a coordinated oxygen atom leading to a $R_2^2(12)$ ring. In the *c* direction the $R_2^1(6)$ motif observed for **7** and **8** is not present, as the comparative oxygen atom acts as acceptor to only one NH group, while the parallel NH group forms a weak bifurcated hydrogen bond with both a sulfur atom and a second uncoordinated oxygen atom on a separate ethylmalonate. The third hydrogen bond is to a coordinated oxygen atom in a third ethylmalonate, and leads to the formation of a $R_2^2(10)$ motif.

The similarities in the hydrogen bonding within these three compounds can be related to the angle between the carboxylate group planes and the distance between the hydrogen-bond acceptors, which are similar for the three compounds. The angle θ between the carboxylate groups is 87° for **7**, 87° for **8** and 88° for **9**, whereas the distance between the oxygen atoms involved in the $R_2^2(10)$ or $R_2^2(11)$ motifs is 3.28 Å for **7**, 3.45 Å for **8** and 3.18 Å for **9**.

The structures adopted by compounds **7**−**9** possess a number of features in common with those previously reported for $[Zn(tu)_2(\mu\text{-phthalate})]_n$ (**4**) and $[Zn(tu)_2(\mu\text{-citraconate})]_n$ (**5**).[14] All of these compounds form helical coordination polymers, which are interlinked by hydrogen bonding in two directions. This is a reflection of the equivalent relative arrangements of the carboxylate within each anion. In **4** and **5**, the carboxylate orientations are determined by the presence of the double bond or benzene ring, and by the steric interactions that prevent co-planarity of the functionalities. In **7**−**9**, the observed carboxylate arrangements are similar to those in **4** and **5**, but in these cases are not dictated by the ligand geometry. Succinate, itaconate and ethylmalonate all contain one or two sp^3-hybridised carbon atoms between the carboxylates, and therefore have the potential of adopting a range of conformations. A search of the Cambridge Structural Database[19] reveals that of the 211 independent $O_2CCH_2CH_2CO_2$ units, 141 (67%) adopt

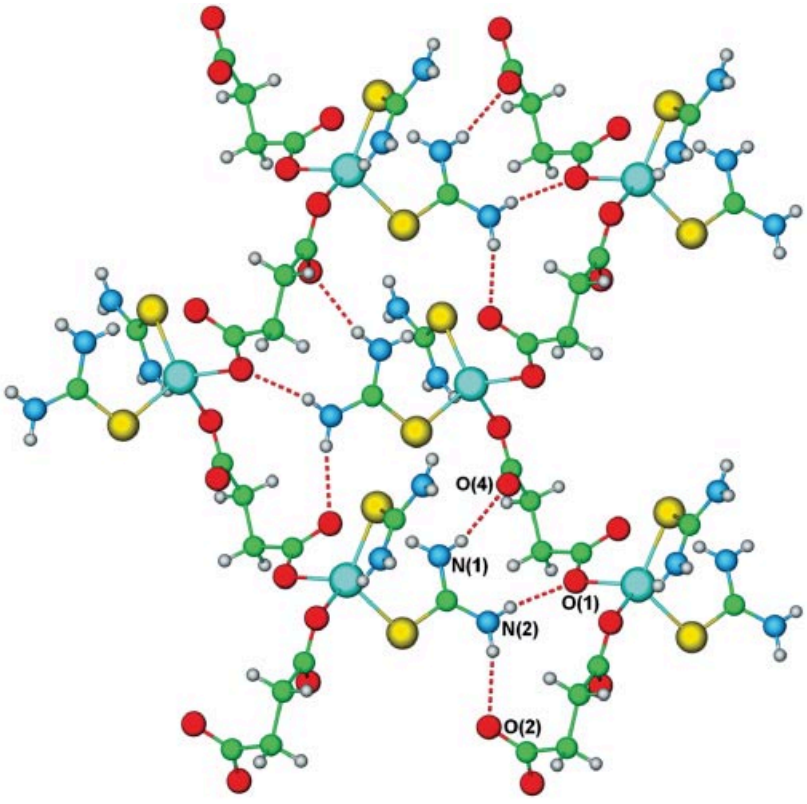

Figure 2. Interchain hydrogen bonding in $[Zn(tu)_2(\mu\text{-succinate})]_n$ (**7**) along the crystallographic *a* axis; selected hydrogen-bond lengths (Å) and angles (°) N(1)···O(4) 3.021, H(1A)···O(4) 2.19, N(1)−H(1A)···O(4) 162; N(2)···O(1) 2.944, H(2A)···O(1) 2.10, N(2)−H(2A)···O(1) 166; and N(2)···O(2) 3.051, H(2B)···O(2) 2.20, N(2)−H(2B)···O(2) 168

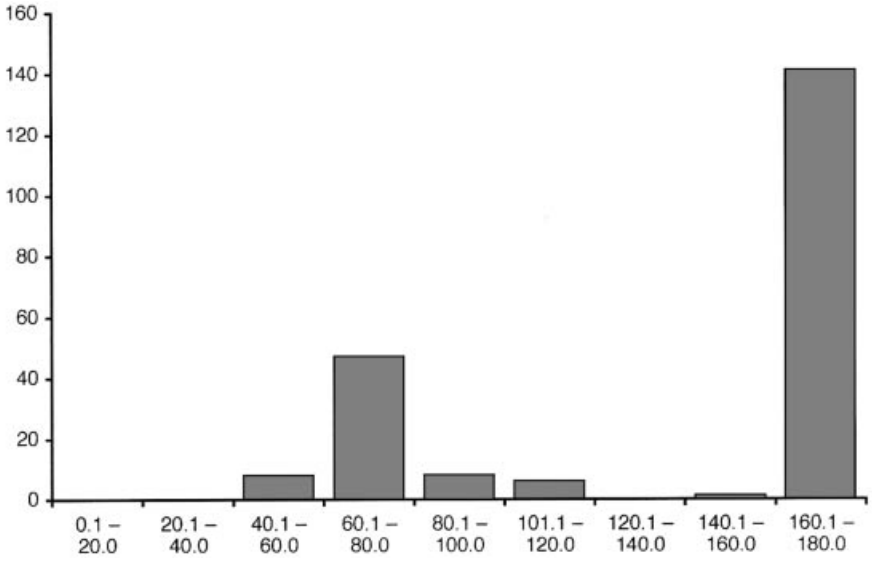

Figure 3. Distribution of CCCC torsion angles in compounds containing the $O_2CCH_2CH_2CO_2$ fragment

an *anti* conformation, with a CCCC torsion angle greater than 160° (Figure 3). In this conformation the O···O distances are all greater than 4.4 Å. In over half of the cases with an O···O distance less than 3.5 Å, this is a direct result of chelation. The observation of helical structures for **7**−**9**, similar to those for **4** and **5**, suggests that this arrangement is driven by the formation of the interhelix hydrogen bonds. The cadmium analogue of **7** has also been reported, and it too has a similar helical structure despite the inclusion of water in the lattice.[20]

The ethylmalonate compound **9** has a very different supramolecular structure to the malonate analogue $[Zn(tu)_2(\mu\text{-malonate})]_n$ (**2**).[14] These differences can be related to the different conformations adopted by the dicar-

boxylates (Figure 4). The steric bulk of the ethyl group and the consequent unfavourable interchain interactions would appear to be the major factor that disfavours **9** from adopting a similar conformation to that observed in **2**.

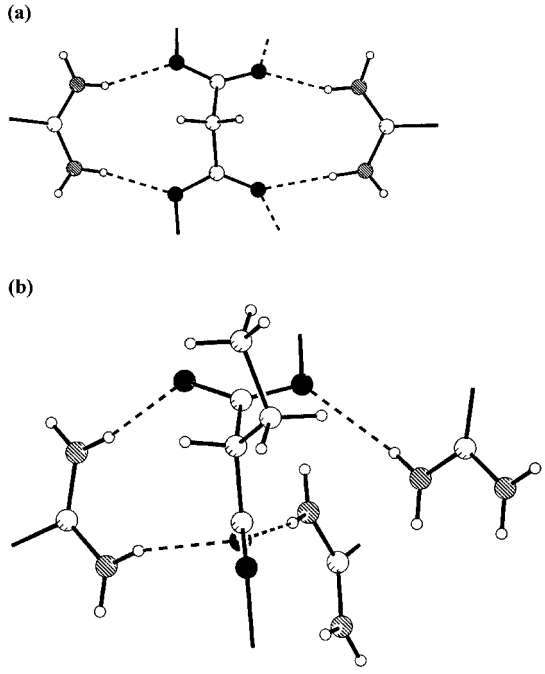

Figure 4. Conformations of and hydrogen bonds to (a) the malonate ligand in **5** and (b) the ethylmalonate ligand in **9**

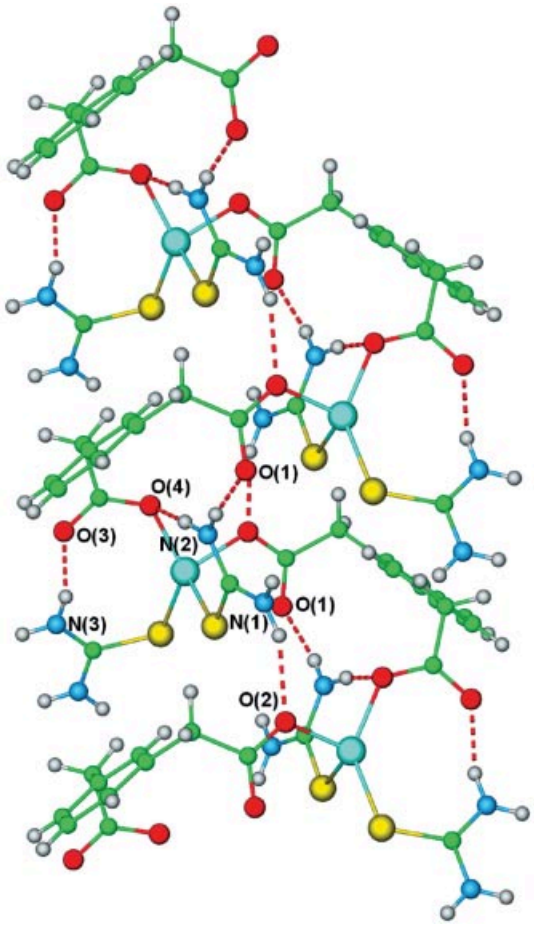

Figure 5. Intrachain hydrogen bonding in one of the independent chains in $[Zn(tu)_2(\mu\text{-}1,3\text{-phenylenediacetate})]_n$ (**10**); selected hydrogen-bond lengths (Å) and angles (°) N(1)···O(2) 2.943, H(1B)···O(2) 2.12, N(1)−H(1B)···O(2) 156; N(2)···O(1) 2.954, H(2A)···O(1) 2.08, N(2)−H(2A)···O(1) 173; N(2)···O(4) 3.011, H(2B)···O(4) 2.17, N(2)−H(2B)···O(4) 160; and N(3)···O(3) 2.756, H(3B)···O(3) 1.90, N(3)−H(3B)···O(3) 163

The Structure of $[Zn(tu)_2(\mu\text{-}1,3\text{-phenylenediacetate})]_n$ (10)

There are two independent helices in the structure of compound **10**, each containing only one of the two crystallographically independent zinc atoms, Zn(1) and Zn(2). Both helical chains contain two intrachain hydrogen bonds between the thiourea NH groups and carboxylate oxygen atoms around each of the zinc centres. These hydrogen bonds involve coordinated and uncoordinated oxygen atoms as acceptors, and give rise to S(6) and S(8) motifs, respectively. This intrachain hydrogen bonding is similar to that observed in **7** and **8**. The length and flexibility of the 1,3-phenylenediacetate ligand allows for additional intrachain hydrogen bonding to more remote thiourea groups. Thus, in each of the independent helices there are two further hydrogen bonds, involving the formation of S(14) and S(16) rings, respectively (Figure 5). One consequence of this additional hydrogen bonding is the increased tightness of the helices, which is reflected in the Zn···Zn···Zn angles, which are 72° and 74° for the two independent polymer chains (93° to 101° for **7**−**9**). The Zn···Zn distances are 6.80 and 6.92 Å for the two chains, shorter than those in **7**−**9**, and clearly illustrate the effect of the intrachain hydrogen bonding. This becomes more apparent when comparing the chains in **10** with those observed in $[Zn\{SC(NHMe)(NH_2)\}_2(\mu\text{-}1,3\text{-phenylenediacetate})]_n$,[21] as in this latter compound, substitution of a hydrogen atom for a methyl group prevents the extended intrachain hydrogen bonding from occurring. Consequently, the Zn···Zn separation is much larger (11.6 Å).

In **10**, the helices are packed in a square-based array rather than in a hexagonal array as observed for **7**−**9**. Each helix interacts, through hydrogen bonds, with helices in the *a* and *ac* directions. In both of these directions there are two hydrogen bonds from parallel NH groups to a single uncoordinated carboxylate oxygen atom, generating $R_2^1(6)$ rings, in addition to one further hydrogen bond, also to an uncoordinated oxygen atom (Figure 6). The hydrogen bonds in both directions link the Zn(1)-based chains to the Zn(2)-based chains. The presence of $R_2^1(6)$ rings with one hydrogen-bond acceptor to the parallel NH groups, as opposed to $R_2^2(n)$ rings with two oxygen atoms acting as acceptors, relates to the distance between oxygen atoms within each dicarboxylate ligand. This O···O distance ranges from 3.18 to 3.45 Å for **7**−**9** but is much longer (5.23 Å) for **10** as a consequence of the greater length of the linker between the carboxylate groups.

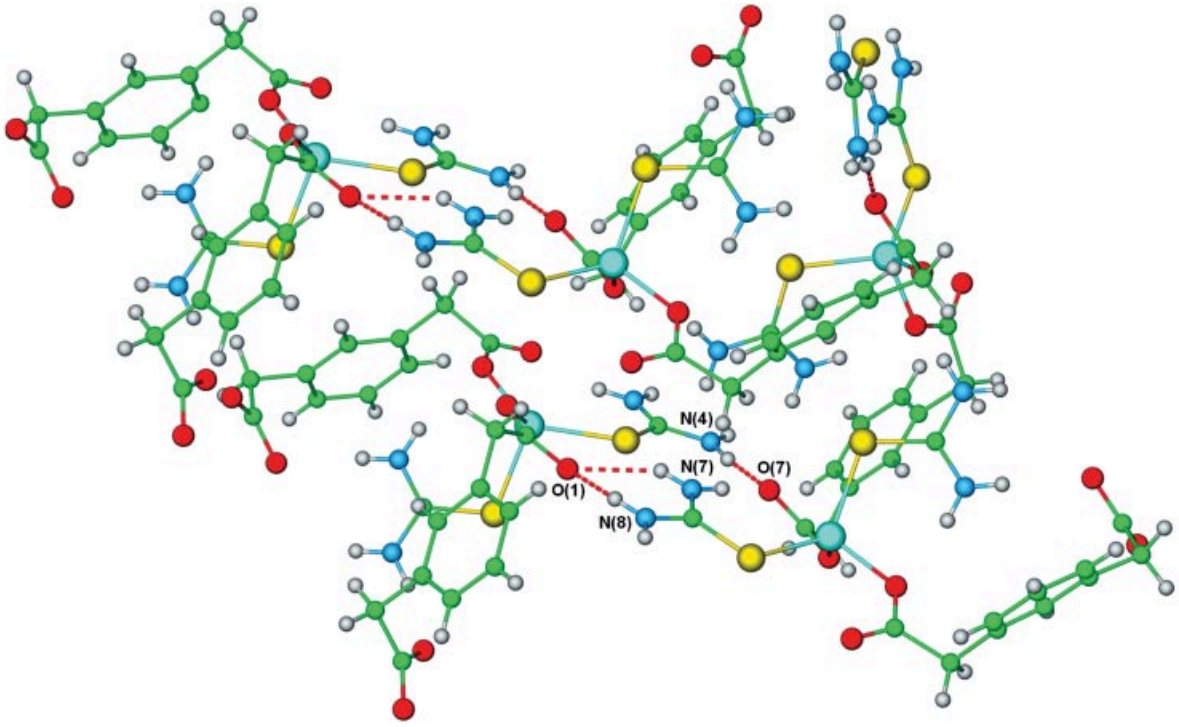

Figure 6. Interchain hydrogen bonding in $[Zn(tu)_2(\mu\text{-}1,3\text{-phenylenediacetate})]_n$ (**10**) along the crystallographic *a* axis; selected hydrogen-bond lengths (Å) and angles (°) N(4)···O(7) 2.935, H(4B)···O(7) 2.06, N(4)−H(4B)···O(7) 173; N(7)···O(1) 2.956, H(7A)···O(1) 2.19, N(7)−H(7A)···O(1) 145; and N(8)···O(1) 2.953, H(8A)···O(1) 2.19, N(8)−H(8A)···O(1) 145

The Structure of $\{[Zn(tu)_2(\mu\text{-mesaconate})]\cdot 2H_2O\}_n$ (11)

In contrast to compounds **7**−**10**, $[Zn(tu)_2(\mu\text{-mesaconate})]_n$ crystallises with two molecules of water per metal centre. Mesaconate has a *trans* arrangement of the carboxylate groups around the central double bond, and consequently the anion is flat. This means that the chains observed in $\{[Zn(tu)_2(\mu\text{-mesaconate})]\cdot 2H_2O\}_n$ (**11**) are not helices, but flat zig-zag chains with a Zn···Zn···Zn angle of 107° and Zn···Zn separations of 8.94 and 9.33 Å. Intrachain hydrogen bonding is observed, and both thiourea ligands are involved in S(6) rings. Only one of the acceptors is an oxygen atom, the other being a sulfur atom (Figure 7). The N−H···S hydrogen bond is, as expected, longer than the N−H···O hydrogen bond, and the Zn−S distance to the sulfur atom involved in the hydrogen bond is the shorter of the two Zn−S distances (Table 1).

Hydrogen bonds involving the two amino protons on a single amino group and an uncoordinated oxygen atom link the chains into a three-dimensional network through the formation of $R_4^2(8)$ rings. All other NH groups are involved in hydrogen bonds with the included water molecules with the exception of N(2)−H(2A), which is involved in a weak N−H···S interaction. The water oxygen atom O(5) acts as a linker between the chains along the crystallographic *b* direction, whereas the water oxygen atom O(6) fulfils the same role along the crystallographic *a* direction.

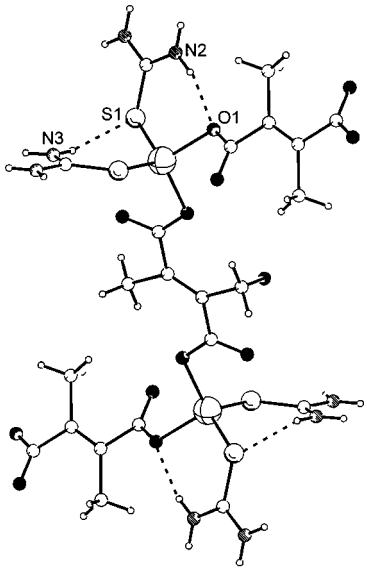

Figure 7. Intrachain hydrogen bonding in $\{[Zn(tu)_2(\mu\text{-mesaconate})]\cdot 2H_2O\}_n$ (**11**); selected hydrogen-bond lengths (Å) and angles (°) N(2)···O(1) 2.916, H(2B)···O(1) 2.06, N(2)−H(2B)···O(1) 163; N(3)···S(1) 3.409, H(3B)···S(1) 2.57, N(3)−H(3B)···S(1) 161; disordered methyl groups are shown in both available positions

Reactions of $[Zn(tu)_4](NO_3)_2$ with Dicarboxylates

The reaction of $[Zn(tu)_4](NO_3)_2$ with a dicarboxylate might be expected to give the same product as that from the reaction of $[Zn(tu)_4]Cl_2$ with the same dicarboxylate. After all, neither chloride nor nitrate is incorporated into the product. Attempts to prepare **1** with $[Zn(tu)_4](NO_3)_2$ suggested that things might not be this simple, and therefore the reactions between $[Zn(tu)_4](NO_3)_2$ and the series of dicarboxylates in Scheme 1 were explored. In the majority

of cases, X-ray powder diffraction studies did indeed verify that the products derived from $[Zn(tu)_4]Cl_2$ and $[Zn(tu)_4](NO_3)_2$ were identical. However, there were two exceptions. The reaction of $[Zn(tu)_4](NO_3)_2$ with terephthalate had previously been reported to give $\{[Zn_2(tu)_2(\mu\text{-tu})(\mu\text{-terephthalate})_2]\cdot 4H_2O\}_n$.[22] In contrast, the analogous reaction with $[Zn(tu)_4]Cl_2$ gave $[Zn(OH_2)_2(\mu\text{-terephthalate})]_n$[23] as the only isolated product. The identity of this compound was confirmed by comparison of the powder X-ray diffraction pattern with that simulated from the single-crystal data. No evidence for thiourea-containing polymers was obtained for this reaction, which is surprising as coordination polymers containing the substituted thioureas $MeNHC(S)NH_2$ and MeNHC(S)NHMe have been prepared in good yield and structurally characterised.[21]

The reaction of $[Zn(tu)_4]Cl_2$ with sodium fumarate was previously reported to give $[Zn(tu)_2(\mu\text{-fumarate})]_n$ (**1**),[14] and this reaction was repeated to confirm **1** as the only product by X-ray powder diffraction. In contrast, the reaction of $[Zn(tu)_4](NO_3)_2$ with sodium fumarate was shown by powder diffraction to give two compounds, **1** and a previously unobserved material. Crystals of the new compound were manually separated from those of **1**, and a single-crystal analysis showed this material to be the hydrated compound $\{[Zn(tu)_2(\mu\text{-fumarate})]\cdot 2H_2O\}_n$ (**12**). Although the reaction with $[Zn(tu)_4]Cl_2$ does not give **12** under normal circumstances, **12** can be isolated as the major product from the reaction by seeding the solution of $[Zn(tu)_4]Cl_2$ and sodium fumarate with small crystals of **12**.

The Structure of $\{[Zn(tu)_2(\mu\text{-fumarate})]\cdot 2H_2O\}_n$ (12)

Like mesaconate, fumarate has a *trans* orientation around the central double bond, and as such the two carboxylate groups are co-planar. Consequently, the coordination polymers formed are flat zig-zag chains as in **11** rather than the helical chains observed for **7**−**10**. There are two intrachain hydrogen bonds around each zinc centre, both involving coordinated oxygen atoms and leading to the formation of S(6) rings (Figure 8). The chains are cross-linked into the three-dimensional structure by three N−H···O hydrogen bonds to carboxylate oxygen atoms and by other interactions involving the included water molecules. Two of the N−H···O hydrogen bonds are to the same acceptor − an uncoordinated oxygen atom − and lead to the generation of an $R_2^1(6)$ motif.

There are a number of key differences in the structures of **1** and **12** brought about by the inclusion of the solvent. The most obvious of these relates to the carboxylate coordination modes (Figure 9). In **1**, the fumarate coordinates in an *anti* coordination mode, which enables it to use the two parallel lone pairs to form DD−AA interactions. This coordination mode is unusual for a carboxylate group, and has not been observed in any other $[Zn(tu)_2(\mu\text{-dicarboxylate})]_n$ structure. In **12**, the carboxylate groups coordinate in the more common manner through *syn* lone pairs. This difference between **1** and **12** affects the distance be-

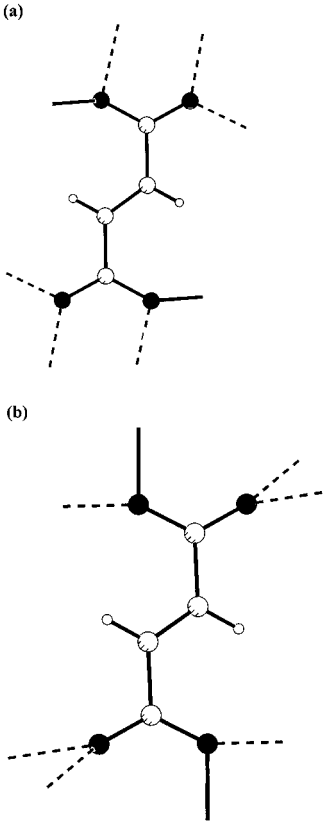

Figure 9. Coordination modes of and hydrogen bonding to the fumarate anions in (a) $[Zn(tu)_2(\mu\text{-fumarate})]_n$ (**1**) and (b) $\{[Zn(tu)_2(\mu\text{-fumarate})]\cdot H_2O\}_n$ (**12**)

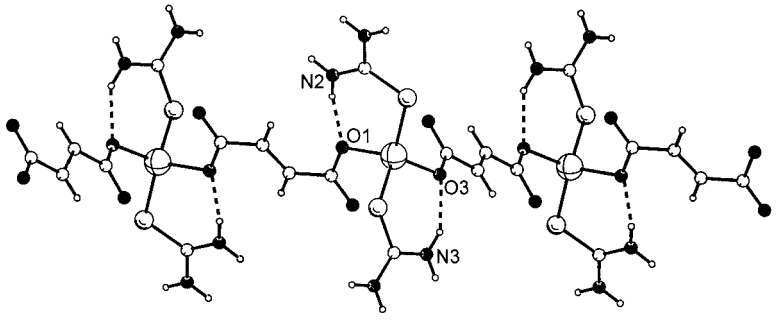

Figure 8. Intrachain hydrogen bonding in $\{[Zn(tu)_2(\mu\text{-fumarate})]\cdot 2H_2O\}_n$ (**12**); selected hydrogen-bond lengths (Å) and angles (°) N(2)···O(1) 2.821, H(2B)···O(1) 1.96, N(2)−H(2B)···O(1) 167; and N(3)···O(3) 2.906, H(3B)···O(3) 2.12, N(1)−H(3B)···O(3) 148

tween Zn centres within the chain and leads to an increase in the Zn···Zn distance from 6.33 Å in **1** to 8.89 and 9.33 Å in **12**. The less favourable coordination mode in **1** is presumably driven by the accompanying DD−AA interactions allowed between the thiourea and carboxylate groups.

The intrachain hydrogen bonds in **1** and **12** also differ. In **1**, sulfur atoms act as acceptors, whereas this role is fulfilled by oxygen atoms in **12**. Both the differing coordination modes of the fumarate and the presence of the water molecules in **12** ensure that the supramolecular structures of **1** and **12** are completely different.

Thermogravimetric Analyses

The presence of the water molecules in compounds **3**, **6**, **11** and **12** begged the question of whether these included molecules could be removed without destruction of the metal-organic frameworks. Consequently, thermogravimetric analyses (TGAs) were carried out on the compounds. The TGA of {[Zn(tu)$_2$(μ-isophthalate)]·H$_2$O} (**3**) showed no mass loss up to 100 °C, followed by a mass loss of 4.5% between 100 °C and 140 °C. This mass loss corresponds to the loss of the water molecule (calcd. 4.51%). The anhydrous material was stable to further mass loss up until 200 °C, at which temperature decomposition started. The anhydrous material **3a** was generated in larger quantities by heating **3** at 150 °C for several hours. Compound **3a** no longer consisted of single crystals, and the X-ray powder diffraction pattern suggested a more fundamental change had occurred than the simple removal of water from the pores within the structure. Compound **3a** does not absorb atmospheric moisture, but can be reconverted into **3** by dissolution in water and reprecipitation. Attempts to prepare other solvates were unsuccessful.

The TGA of {[Zn(tu)$_2$(μ-maleate)]·H$_2$O} (**6**) showed no mass loss until 150 °C. A gradual loss of mass until 270 °C was then observed, followed by more rapid mass loss on destruction of the framework. Water comprises 5.1% of **6**, although a mass less than this had been lost up to 270 °C. The TGA of {[Zn(tu)$_2$(μ-mesaconate)]·2H$_2$O} (**11**) showed no mass loss until 120 °C and only a gradual loss of 2% until the start of decomposition of the framework at 250 °C. The TGA of {[Zn(tu)$_2$(μ-fumarate)]·2H$_2$O} (**12**) revealed a mass loss between 50 and 120 °C corresponding to the elimination of the included water molecules. The resulting anhydrous product was then stable up to 220 °C, after which it began to lose mass again. This second mass loss corresponds to the destruction of the metal-organic framework. The X-ray powder diffraction pattern of **12** changed markedly on solvent loss and is different from that of **1**.

These results imply a different structural role for the water molecules in **3** and **12** relative to that in **6** and **11**. The higher temperature at the onset of mass loss, combined with the absence of a clearly defined anhydrous compound for **6** and **11**, suggest that the water is an integral part of the supramolecular structure. This is consistent with the structural data that show the water as being part of the hydrogen-bonding networks in **6** and **11**. In contrast, water loss occurs at lower temperatures for **3** and **12**, and the anhydrous compounds are stable over a wide temperature range. This indicates that the water molecules play a less important structural role in these compounds. This is certainly true for **3**, in which the water molecules are disordered and lie within pores in the structure. In **12**, the water molecules lie within channels along the crystallographic 111 direction. The majority of the hydrogen bonding involves O−H···O and O−H···S interactions, which suggests that these water molecules are less well-bound than those in **11**, as confirmed by the TGA experiments.

TGA on the anhydrous compounds **1**, **4**−**5** and **7**−**10** showed no significant mass loss until the onset of decomposition of the framework between 180 °C and 230 °C. In contrast, [Zn(tu)$_2$(μ-malonate)]$_n$ **2** lost 9.5% of mass between 80 °C and 200 °C. This corresponds to a mass of 30, and it is difficult to rationalise such a mass loss at the current time.

Conclusions

The crystal structures for compounds **7**−**9** provide good evidence that the structures based on helical polymers interlinked by hydrogen bonding, previously observed for [Zn(tu)$_2$(μ-citraconate)]$_n$ and [Zn(tu)$_2$(μ-phthalate)]$_n$, represent recurrent motifs. This is a favourable product for cases in which the dicarboxylate can adopt an orientation with mutually perpendicular carboxylate planes, and O···O separations between 3 and 3.5 Å. The crystal structure for **12** is surprising as it demonstrates that the [Zn(tu)$_4$]X$_2$ anion, despite not being incorporated into the final product, plays a role in determining the nature of the product. The chloride compound exclusively gives [Zn(tu)$_2$(μ-fumarate)]$_n$ (**1**), whereas the nitrate analogue gives both **1** and {[Zn(tu)$_2$(μ-fumarate)]·H$_2$O}$_n$ (**12**). The chloride anion has a greater coordinating nature than the nitrate anion, and the previous observation of compounds such as [ZnCl$_2${SC(NHMe)(NMe$_2$)}$_2$] from the reaction of [Zn{SC(NHMe)(NMe$_2$)}$_4$]Cl$_2$ and a dicarboxylate,[24] suggests that the reactive species in solution from [Zn(tu)$_4$]Cl$_2$ may be [ZnCl$_2$(tu)$_2$] rather than [Zn(tu)$_4$]$^{2+}$. It is possible that this affects the solution concentration of intermediates such as [Zn(tu)$_2$(dicarboxylate)$_2$]$^{2-}$, which in turn may influence the crystallisation route adopted. However, no evidence for the intermediates was observed by NMR spectroscopy, and therefore such inferences should be regarded as speculative at this stage.

Experimental Section

General Remarks: Microanalyses (C, H and N) were carried out by Mr. Alan Carver (University of Bath Microanalytical Service). Infrared spectra were recorded with a Nicolet Nexus FT-IR spectrometer as KBr pellets, and thermogravimetric analyses were carried out with a Perkin−Elmer TGA 7 instrument. [Zn(tu)$_4$]Cl$_2$,[25] [Zn(tu)$_4$](NO$_3$)$_2$[26] and compounds **1**−**6**[14] were prepared as described in the literature. Sodium dicarboxylates were prepared by

reaction of the appropriate dicarboxylic acid with either sodium hydroxide or sodium hydrogen carbonate.

Synthesis of [Zn(tu)$_2$(μ-succinate)]$_n$ (7): An aqueous solution of sodium succinate (0.037 g, 0.23 mmol) was added to an aqueous solution of [Zn(tu)$_4$]Cl$_2$ (0.10 g, 0.23 mmol), with no discernible change. After several days a colourless crystalline precipitate was observed, which was separated by filtration. Yield 0.059 g (78%). $C_6H_{12}N_4O_4S_2Zn$ (333.7): calcd. C 21.6, H 3.62, N 16.8; found C 21.6, H 3.63, N 17.0. IR: $\tilde{\nu}$ = ν(NH) 3454 s; ν(CO$_2$)/δ(NH$_2$) 1658 s, 1584 s, 1504 s cm^{-1}.

Compounds **8**−**11** were prepared in an analogous manner to **1** with [Zn(tu)$_4$]Cl$_2$ (0.10 g, 0.23 mmol) and one equivalent of the appropriate sodium dicarboxylate.

[Zn(tu)$_2$(μ-itaconate)]$_n$ (8): Yield 0.053 g (68%). $C_7H_{12}N_4O_4S_2Zn$ (345.7): calcd. C 24.3, H 3.50, N 16.2; found C 24.2, H 3.48, N 16.1. IR: $\tilde{\nu}$ = ν(NH) 3447 s, 3368 s, 3321 s, 3208 s (br); ν(CO$_2$)/δ(NH$_2$) 1644 s, 1577 m, 1511 s, 1384 m cm^{-1}.

[Zn(tu)$_2$(μ-ethylmalonate)]$_n$ (9): Yield 0.057 g (72%). $C_7H_{14}N_4O_4S_2Zn$ (347.7): calcd. C 24.2, H 4.06, N 16.1; found C 24.1, H 3.99, N 16.0. IR: $\tilde{\nu}$ = ν(NH) 3408 s (br), 3327 s (br), 3195 s (br); ν(CO$_2$)/δ(NH) 1637 s, 1584 s (br), 1358 m cm^{-1}.

[Zn(tu)$_2$(μ-1,3-phenylenediacetate)]$_n$ (10): Yield 0.049 g (53%). $C_{12}H_{16}N_4O_4S_2Zn$ (409.8): calcd. C 35.2, H 3.94, N 13.7; found C 35.1, H 3.90, N 13.5. IR: $\tilde{\nu}$ = ν(NH) 3311 s (br), 3197 s (br); ν(CO$_2$)/δ(NH$_2$) 1659 s, 1640 s, 1563 s, 1511 s, 1370 s (br) cm^{-1}.

{[Zn(tu)$_2$(μ-mesaconate)]·2H$_2$O}$_n$ (11): Yield 0.059 g (76%). $C_7H_{12}N_4O_4S_2Zn$ (345.7): calcd. C 24.3, H 3.50, N 16.2; found C 21.6, H 3.63, N 17.0. IR: $\tilde{\nu}$ = ν(NH) 3394 s (br), 3142 s (br); ν(CO$_2$)/δ(NH$_2$) 1644 s, 1557 s, 1511 s, 1438 s, 1345 m cm^{-1}.

Synthesis of {[Zn(tu)$_2$(μ-fumarate)]·2H$_2$O}$_n$ (12): An aqueous solution of sodium fumarate (0.032 g, 0.20 mmol) was added an aqueous solution of [Zn(tu)$_4$](NO$_3$)$_2$ (0.100 g, 0.20 mmol), with no discernible change. After several hours a colourless crystalline precipitate was observed, which was separated by filtration. Yield 0.058 g (78%). $C_6H_{10}N_4O_4S_2Zn$ (331.7): calcd. C 19.6, H 3.81, N 15.2; found C 19.6, H 3.52, N 15.1. IR: $\tilde{\nu}$ = ν(NH)/OH 3421 s, 3374 s, 3301 s, 3182 s, 3135 s; ν(CO$_2$)/δ(NH$_2$) 1624 s, 1565 d, 1511 s, 1371 s (br) cm^{-1}.

Single crystals of compounds **7**−**12** suitable for X-ray analysis were obtained by repeating the reactions on a smaller scale in a more dilute solution, allowing the crystals to grow over several days. Compounds **2**−**11** were also prepared from [Zn(tu)$_4$](NO$_3$)$_2$, and their identities confirmed by X-ray powder diffraction studies.

Crystallography: Single crystals of the compounds **7**, **8**, **9** and **11** were analysed with an Enraf−Nonius CAD4 diffractometer, while data for **10** and **12** were collected with a Nonius KappaCCD diffractometer. Graphite-monochromated Mo-K_α radiation was employed throughout. Details of the data collections, solutions and refinements are given in Table 3. The structures were solved using SHELXS-97[27] and refined using SHELXL-97.[28] Absorption corrections (semi-empirical from equivalent reflections) were applied to data for **10** and **12**. (Max./min. transmission factors 0.82, 0.62 and 1.000, 0.890, respectively). Hydrogen atoms were universally included at calculated positions except in solvent water molecules, where they were located in the penultimate difference Fourier electron-density maps and restrained at 0.89 Å from the relevant parent oxygen. Convergence was routine throughout, with the exception of the observations below.

Positional disorder (65:35) was observed in the ethyl group of the ethylmalonate ligand in **9**. In the final least-squares refinement, the ADPs for the alpha carbon partial atoms [C(6), C(6A)] were restrained to be similar, while those for C(7) and C(7A) were constrained to be identical. The asymmetric unit in **10** was seen to be based on two independent zinc centres.

The asymmetric unit in **11** contained two solvent water molecules for each zinc centre. The metal is sulfur-bound to two thiourea units and oxygen-bound to two crystallographically independent anion halves. The proximity of the anion halves to inversion centres means that the single methyl group contained in each is disordered in a 1:1 ratio between the two available positions for its location. The water hydrogen atoms on O(6) could not be reliably located, and hence were omitted from the refinement. The asymmetric unit for **12** closely parallels that for **11** insofar as it contains two solvent water molecules for each zinc centre. The coordination sphere around the metal is similar, and also consists of two anion halves

Table 3. Crystallographic information for compounds **7**−**12**

	7	**8**	**9**	**10**	**11**	**12**
Empirical formula	$C_6H_{12}N_4O_4S_2Zn$	$C_7H_{12}N_4O_4S_2Zn$	$C_7H_{14}N_4O_4S_2Zn$	$C_{24}H_{32}N_8O_8S_4Zn_2$	$C_7H_{15}N_4O_6S_2Zn$	$C_6H_{14}N_4O_6S_2Zn$
M	333.69	345.70	347.71	819.56	380.72	367.70
Crystal system	orthorhombic	orthorhombic	orthorhombic	monoclinic	triclinic	triclinic
Space group	$P2_12_12_1$	$P2_12_12_1$	$P2_12_12_1$	$P2_1/c$	$P\bar{1}$	$P\bar{1}$
a (Å)	8.3080(10)	8.327(2)	8.331(2)	18.8080(3)	7.1377(6)	7.7910(2)
b (Å)	11.2380(10)	11.742(2)	10.778(2)	8.1800(1)	8.616(1)	8.5230(2)
c (Å)	13.5350(10)	13.396(4)	15.209(6)	21.2960(4)	12.658(5)	10.9450(2)
a (°)	90	90	90	90	102.42(1)	91.105(1)
β (°)	90	90	90	98.197(1)	91.176(9)	102.602(1)
γ (°)	90	90	90	90	92.661(8)	97.949(1)
V (Å^3)	1263.7(2)	1309.7(5)	1365.6(7)	3242.91(9)	759.0(3)	701.53(3)
Z	4	4	4	4	2	2
μ (mm^{-1})	2.282	2.205	2.115	1.796	1.920	2.074
Reflections collected	1330	1264	1296	32037	2973	2852
Independent reflections	1288	1110	1209	7406	2652	2819
R(int.)	0.0105	0.0094	0.0076	0.0671	0.0131	0.0238
*R*1, *wR*2 [$I > 2\sigma(I)$]	0.0391, 0.0971	0.0277, 0.0735	0.0488, 0.1243	0.0348, 0.0723	0.0424, 0.1118	0.0464, 0.1247
R indices (all data)	0.0421, 0.0988	0.0332, 0.0764	0.0523, 0.1271	0.0533, 0.0794	0.0432, 0.1121	0.0467, 0.1248

proximate to crystallographic inversion centres in addition to a pair of thiourea ligands. The hydrogen atoms in the water molecule based on O(5) in this structure could not be reliably located and were omitted from the refinement.

CCDC-241267 to -241272 for compounds **7**−**12** contains the supplementary crystallographic data for this paper. These data can be obtained free of charge at www.ccdc.cam.ac.uk/conts/retrieving.html [or from the Cambridge Crystallographic Data Centre, 12 Union Road, Cambridge CB2 1EZ, UK; Fax: +44-1223-336-033; E-mail: deposit@ccdc.cam.ac.uk].

Supporting Information: Figures showing the interchain hydrogen bonding in compounds **7**, **11** and **12** are available (see also footnote on the first page of this article).

Acknowledgments

The EPSRC is thanked for financial support.

[1] A. D. Burrows, *Struct. Bond.* **2004**, *108*, 55−95.
[2] T. Steiner, *Angew. Chem. Int. Ed.* **2002**, *41*, 48−76.
[3] C. B. Aakeröy, A. M. Beatty, *Aust. J. Chem.* **2001**, *54*, 409−421.
[4] A. D. Burrows, C.-W. Chan, M. M. Chowdhry, J. E. McGrady, D. M. P. Mingos, *Chem. Soc., Rev.* **1995**, *24*, 329−339.
[5] M. Tadokoro, H. Kanno, T. Kitajima, H. Shimada-Umemoto, N. Nakanishi, K. Isobe, K. Nakasuji, *Proc. Natl. Acad. Sci. USA* **2002**, *99*, 4950−4955.
[6] U. Suksangpanya, A. J. Blake, P. Hubberstey, C. Wilson, *CrystEngComm* **2002**, *4*, 638−643.
[7] L. R. Falvello, R. Garde, M. Tomás, *Inorg. Chem.* **2002**, *41*, 4599−4604.
[8] S. L. James, *Chem. Soc., Rev.* **2003**, *32*, 276−288.
[9] C. Janiak, *Dalton Trans.* **2003**, 2781−2804.
[10] R. Robson, *J. Chem. Soc., Dalton Trans.* **2000**, 3735−3744.
[11] A. D. Burrows, R. W. Harrington, M. F. Mahon, S. J. Teat, *Eur. J. Inorg. Chem.* **2003**, 766−776.
[12] J. E. V. Babb, A. D. Burrows, R. W. Harrington, M. F. Mahon, *Polyhedron* **2003**, *22*, 673−686.
[13] A. D. Burrows, R. W. Harrington, M. F. Mahon, S. J. Teat, *Cryst. Growth Des.* **2004**, *4*, 813−822.
[14] A. D. Burrows, R. W. Harrington, M. F. Mahon, C. E. Price, *J. Chem. Soc., Dalton Trans.* **2000**, 3845−3854.
[15] Y. Zhang, J. Li, J. Chen, Q. Su, W. Deng, M. Nishiura, T. Imamoto, X. Wu, Q. Wang, *Inorg. Chem.* **2000**, *39*, 2330−2336.
[16] Y. Zhang, J. Li, M. Nishiura, H. Hou, W. Deng, T. Imamoto, *J. Chem. Soc., Dalton Trans.* **2000**, 293−297.
[17] Y. Ke, J. Li, Y. Zhang, *Cryst. Res. Technol.* **2002**, *37*, 501−508.
[18] J. Bernstein, R. E. Davis, L. Shimoni, N.-L. Chang, *Angew. Chem. Int. Ed. Engl.* **1995**, *34*, 1555−1573.
[19] D. A. Fletcher, R. F. McMeeking, D. Parkin, *J. Chem. Inf. Comput. Sci.* **1996**, *36*, 746−749.
[20] Y. Zhang, J. Li, M. Nishiura, W. Deng, T. Imamoto, *Chem. Lett.* **1999**, 1287−1288.
[21] N. J. Burke, A. D. Burrows, A. S. Donovan, R. W. Harrington, M. F. Mahon, C. E. Price, *Dalton Trans.* **2003**, 3840−3849.
[22] A. D. Burrows, S. Menzer, D. M. P. Mingos, A. J. P. White, D. J. Williams, *J. Chem. Soc., Dalton Trans.* **1997**, 4237−4240.
[23] G. Guilera, J. W. Steed, *Chem. Commun.* **1999**, 1563−1564.
[24] A. D. Burrows, R. W. Harrington, M. F. Mahon, unpublished results.
[25] S. J. Ashcroft, *J. Chem. Soc., A* **1970**, 1020−1024.
[26] R. Vega, A. López-Castro, R. Márguez, *Acta Crystallogr., Sect. B* **1978**, *34*, 2297−2299.
[27] G. M. Sheldrick, *Acta Crystallogr., Sect. A* **1990**, *46*, 467−473.
[28] G. M. Sheldrick, *SHELXL-97, Computer Program for Crystal Structure Refinement*, University of Göttingen, **1997**.

Received June 10, 2004
Early View Article
Published Online October 14, 2004

